A pH-Responsive Cu-Corrole-Based Cage That Reversibly Encapsulates Fullerene in a Shapeshifting Low-Symmetry Cavity

Anna Baidiuk, Tània Pèlachs, Paul-Gabriel Julliard, György Szalóki, Marc Vedrenne, Xavi Ribas, Maylis Orio, Alexandre Martinez, Gabriel Canard, Cédric Colomban

A pH-Responsive Cu-Corrole-Based Cage that Reversibly Encapsulates Fullerene in a Shapeshifting Low-Symmetry Cavity.

Anna Baidiuk,[a] Tània Pèlachs,[b] Paul-Gabriel Julliard,[c] György Szalóki,[d] Marc Vedrenne,[d] Xavi Ribas,[b] Maylis Orio,*[a] Alexandre Martinez,*[a] Gabriel Canard,*[c] and Cédric Colomban*[a].

[a] Aix Marseille Université, CNRS, Centrale Méditerranée, iSm2 (UMR 7313), 13013 Marseille, France.

[b] Institut de Quimica Computacional i Catalisi, Departament de Quimica. Universitat de Girona, E-17003 Girona, Spain

[c] Aix Marseille Université, CNRS, CINAM (UMR 7325), Campus de Luminy, 13288 Marseille cedex 09, France.

[d] Université de Toulouse, CNRS, LHFA (UMR 5069), 118 Route de Narbonne, 31062 Toulouse Cedex 09, France.

KEYWORDS. Low-symmetry molecular cages • Stimuli-responsive systems • Adaptable host • Fullerene • Corrole cages.

ABSTRACT: Artificial hosts combining chemical functionalities (recognition sites, stimuli responsive behavior) in a low-symmetrical and guest-adaptive environment, are of major interest to better understand and mimic protein receptors. However, molecular cages are generally restricted to symmetrical cavities built from rigid subunits. For instance, porphyrin building blocks have a time-honored role in the preparation of receptors and confined catalysts. Here, we introduce a new design for molecular cages based on corroles, the low symmetrical analogue of porphyrins, breathing life to desymmetrized cavities. A (Cu^{III})corrole complex was equipped with a shapeshifting cyclotriveratrylene (CTV) roof, *via* pH-responsive side arms. The latter enables the first metallocorrole-based cage Cu^{III}(**Hm-Cor**) to reversibly bind fullerenes in a unique low-symmetry, conformationally adaptive, and pH-responsive cavity. Experimental and computational studies evidence flipping of the CTV roof upon fullerene binding, enabling structural reconfiguration of the host to adapt its size and shape to selectively accommodate the guest. Such conformational change also responds to the protonation of the cage's side-arms. This pH-responsive cavity allows fullerene release and reuse of the host. Beyond establishing a key precedent for preparation of caged metallocorroles, the present study provides a unique approach for the on-demand fullerenes encapsulation in a low symmetry environment enabling precise positioning of the guest and control over its functionalization.

INTRODUCTION

The field of cage-like artificial receptors has rapidly expanded in recent years. Either covalent or self-assembled cages have found emerging applications in sensing, separation, delivery and catalysis in confined space.[1] However, when comparing current artificial hosts to their natural paradigms - protein-based receptors - one realizes that their complexity still differs widely. Biological receptors achieve efficient and highly selective substrate complexation by means of sophisticated hosts combining recognition and reaction sites in low-symmetrical and conformationally adaptive cavities.[2] In contrast, synthetic molecular cages generally display highly symmetric cavities built from rigid building blocks, associated to simpler preparations and characterizations.[3] Interests in desymmetrized cage compounds,[4] guest-adaptive shapeshifting cavities,[5] and stimuli responsive hosts for controlled guest release,[6] are therefore increasing rapidly. However, the quest for cage design combining these features, remains one of the greatest challenges.[7]

Porphyrin derivatives are part of the most widely used building blocks of either self-assembled or covalent molecular cages,[8] applied in both catalysis[9] and host-guest chemistry.[10] In particular, metalloporphyrin units and fullerene guests are engaged in a long-standing relationship enabling stable host-guest complexes with high association constants (*via* strong π-π or donor-acceptor interactions).[11] Fullerene chemistry has recently benefited from porphyrin-based supramolecular shadow masks allowing remarkable selective functionalization.[12]

Could challenging heme-like hosts with desymmetrized cavity be prepared by integrating low symmetrical porphyrin analogues?

In this context, the emerging metallocorroles are "contracted" heme-like tetrapyrrolic compounds,[13] with versatile range of applications, from metalloprotein modelling to small molecule activation catalysis.[14] The appealing corrole-based building blocks differ from porphyrins due to their contracted core with reduced (C_{2V}) symmetry and their unique tri-*meso* substitution. [15] However, reported cases of three-dimensionally functionalized corroles are few,[16,17,18] and corrole-based cage-receptors remain so far unexplored.

Here, we report a novel design of porphyrinoid molecular cage based on a low-symmetrical metallocorrole foundation equipped with three pH-responsive side-walls and a concave cyclotriveratrylene (CTV) roof, which can adopt inward or outward conformations. We uncover the key to unlock the preparation of the first metallocorrole cage Cu^{III}(**Hm-Cor**): the inherently saddle geometry of the Cu^{III}(corrole) core that allows free rotation of all *meso* side arms. Both CTV and metallocorrole recognition units enable Cu^{III}(**Hm-Cor**) to bind fullerenes in a unique cavity displaying three non-equivalent apertures allowing precise guest positioning. The corrole host also undergoes a remarkable conformational change between closed and open states, that respond to the presence of fullerene guests and to the protonation of the cage's side-arms (Figure 1). We show how the pH-responsive, shape-shifting cavity can lead to the on-demand uptake and release of fullerene, providing a reusable host.

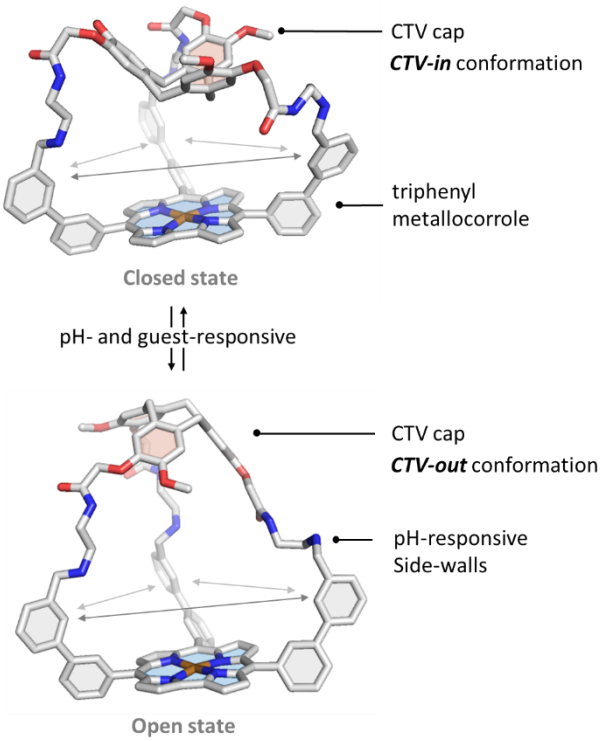

Figure 1. Representation of the interconversion between the *CTV-in* and the stimuli-driven *CTV-out* conformations of the corrole-based cage Cu^{III}(**Hm-Cor**) displaying non-equivalent apertures.

RESULTS AND DISCUSSION

Design, Synthesis and Characterization of Cu^{III}(Hm-Cor). Creation of a heme-like fullerene host combining low-symmetry with conformational adaptivity (responding to external stimulus), required functionalization of the corrole core with a conformationally switchable fullerene recognizing unit. We therefore designed the hemicryptophane Cu^{III}(**Hm-Cor**), where the archetypal triphenylcorrole (**TPCor**) ligand is covalently linked to a northern CTV unit *via* three amine bridges (Figure 1). The northern CTV cap and southern **TPCor**, that serve as "roof" and "floor" respectively, both offer large π-surfaces designed to act as fullerene recognition sites. Beyond being well-adapted to the *tris-meso* substitution of corroles, the tripodal CTV could serve as a guest-adaptive conformationally switchable unit since (*i*) temperature- and solvent-dependent concave–convex switching of the CTV was recently observed in cryptophane,[19] and hemicryptophane cages,[20] and (*ii*) shape complementarity between fullerenes and the concave CTV surface is particularly suited to establish concave-convex π-π interactions.[21] Finally, the three amine-based "side-walls" were designed to serve as pH-responsive units.[6a] The synthetic strategy combines a triple Suzuki-Miyaura-based functionalization of the **TPCor** core (introducing three phenylcarboxaldehyde moieties), with formation of the cage in a final 1+1 reductive amination step with the amine-based **CTV-1** (Figure 2). The 3-carboxaldehyde units were introduced at the *meta*-position of the corrole's *meso*-aryl substituents, aiming at favouring free rotation and avoiding atropoisomers. This was obtained *via* functionalization of the reported brominated corrole **1**,[22] by triple Suzuki-Miyaura cross coupling with the 3-formylphenylboronic acid (Figure 2a), forming the aldehyde-based corrole **2** with 42% yield. However, ^{1}H NMR spectrum of the free base corrole **2** displays broad resonances that might account for restricted rotation of the biphenyl arms (Figure S2). The latter might be detrimental to the formation of the target cage by favouring the formation of polymeric species over discrete compounds. Indeed, no formation of the targeted cage could be observed upon reaction of the free base corrole **2** with **CTV-1** under reductive amination conditions. This reaction leads, instead, to the formation of insoluble material. We then reasoned that metalation of **2** with the copper ion might allow free rotation of the three biphenyl-3-carboxaldehyde units. Copper(III) *meso*-triarylcorroles indeed display a peculiar saddle geometry that might favour rotation of the *meso*-substituents by enhancing the "breathing ability" of the corrole core.[23] As anticipated, ^{1}H NMR spectrum of Cu^{III}(**2**) displays sharp and well defined resonances for both the *β*-pyrrole-protons of the macrocycle and its *meso* substituents, evidencing free rotation of the biphenyl side-arms (Figures S5-S7). Pleasingly, its 1+1 coupling with the amine-based **CTV-1** leads to the formation of the target cage Cu^{III}(**Hm-Cor**) with remarkably high yield (90%).[24] Isolation of Cu^{III}(**Hm-Cor**) with high yield allows for reporting the structural key for corrole cage formation, namely the metal-responding corrole geometry that governs free rotation of the *meso* side-arms. The first metallocorrole cage Cu^{III}(**Hm-Cor**), was fully characterized by means of high-resolution mass spectrometry (ESI-HRMS), cyclic voltammetry, UV-vis and 1D and 2D NMR spectroscopies.

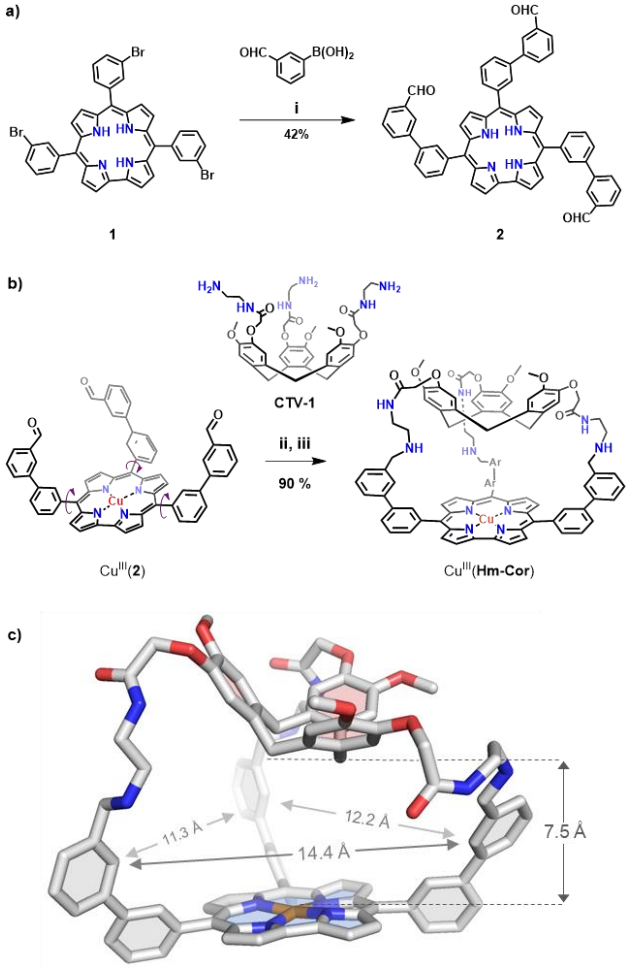

Figure 2. (**a**) Synthesis of the biphenyl-3-carboxaldehyde-based corrole **2**. (**b**) Preparation and (**c**) DFT-optimized structure of the corrole-based cage Cu^{III}(**Hm-Cor**). Experimental conditions: (**i**) $Pd(PPh_3)_4$, Cs_2CO_3, toluene/MeOH/H_2O 2:1:2, Ar, 100°C, 48 h; (**ii**) MeOH/$CHCl_3$ 1:1, 75°C, 72 h; (**iii**) $NaBH_4$, rt, 3 h.

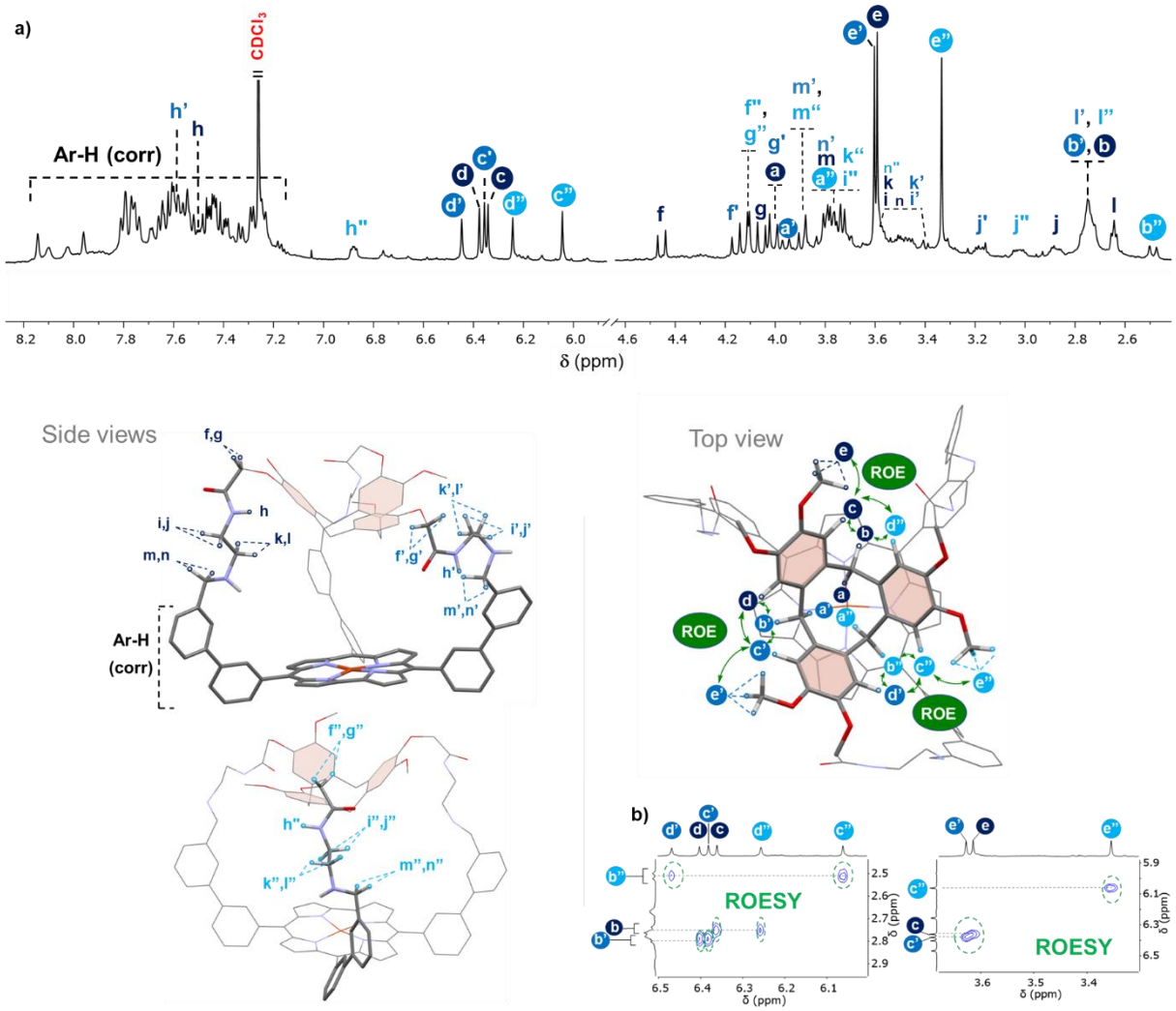

Figure 3. (**a**) ^{1}H NMR spectrum ($CDCl_3$, 500 MHz, 298 K) of Cu^{III}(**Hm-Cor**) along with side (front and back) and top views of its DFT-optimized structure. (**b**) Partial ROESY spectra ($CDCl_3$, 600 MHz, 298 K) of Cu^{III}(**Hm-Cor**) showing the relevant cross-peaks for assignment of the signals belonging to the CTV cap (circle letters labels).

ESI-HRMS analysis of Cu^{III}(**Hm-Cor**) revealed three sets of signals corresponding to its *mono*, *bis* and *tris* protonated adducts (Figure S9). The UV-vis spectrum of Cu^{III}(**Hm-Cor**) in CH_2Cl_2 displays the typical Soret (413 nm, ε = 82925 M^{-1} cm^{-1}) and Q-bands (542 and 618 nm, ε = 8002 and 5373 M^{-1} cm^{-1} respectively), fingerprints of the Cu^{III}(corrole) core, along with the typical CTV absorbance in the 290 - 300 nm region (Figure S10). Cyclic voltammogram of Cu^{III}(**Hm-Cor**), displays the typical reversible reduction process at -680 mV vs $Fc^{+/0}$, attributed to metal-centered reduction (Cu^{III}/Cu^{II}, Figure S11). The ^{1}H NMR spectrum of Cu^{III}(**Hm-Cor**) reveals an overall C_1 symmetry with magnetically inequivalent side-arms confirming its low-symmetry. Although split, the ^{1}H NMR spectrum of Cu^{III}(**Hm-Cor**) displays remarkably sharp and well-defined signals for the protons belonging to the CTV roof ($H_{a,a',a''}$; $H_{b,b',b''}$; $H_{c,c',c''}$; $H_{d,d',d''}$; $H_{e,e',e''}$), and to the linkers ($H_{f,f',f''}$; $H_{g,g',g''}$; $H_{h,h',h''}$; $H_{i,i',i''}$; $H_{j,j',j''}$; $H_{k,k',k''}$; $H_{l,l',l''}$; $H_{m,m',m''}$; $H_{n,n',n''}$), that have been successfully assigned through 2D NMR experiments (Figures S16 and S17). Each proton shows distinct resonances, with the two opposite "side-walls" displaying slightly shifted resonances while protons belonging to the third arm display more shifted signals ($H_{a''-n''}$, Figure 3). ^{1}H-DOSY (diffusion order spectroscopy) NMR analysis of Cu^{III}(**Hm-Cor**) confirms that all signals assigned to Cu^{III}(**Hm-Cor**) have identical diffusion coefficient *D* of $4.9.10^{-10}$ $m^2.s^{-1}$ (Figure S18a). Importantly, signals belonging to the aromatic protons of the CTV unit ($H_{c,c',c''}$ and $H_{d,d',d''}$), that resonate as six distinct singlets between 6.04 ppm and 6.45 ppm, experience an intense upfield-chemical shift compared to usual "*CTV-out*" hemicryptophane cages,[25] or to open CTV derivatives such as **CTV-1**, in which these protons resonate in the 6.7 to 6.9 ppm region (Figure S19). Similarly, other signals belonging to the CTV unit, the O-**CH_3** protons ($H_{e,e',e''}$ 3.3 - 3.6 ppm) and the axial ($H_{a,a',a''}$ 3.8 - 4.0 ppm) and equatorial ($H_{b,b',b''}$ 2.5 - 2.8 ppm) methylenic bridging protons, undergo strong upfield-chemical shifts compared to **CTV-1**. Interestingly, the strong upfield shift of the CTV resonances are in perfect agreement with previous reports of capsules displaying the so called "*CTV-in*" conformation where the convex CTV surface is pointing toward the inside of the cavity. It was indeed demonstrated, by us and other groups, that *CTV-in* conformations in cryptophanes,[19] and hemicryptophanes,[20] display the specific chemical shifts observed in Cu^{III}(**Hm-Cor**). The rather wide *tris*-phenyl-corrole platform associated to flexible -CH_2-CONH-C_2H_4-NH-CH_2- linkers, and the electronic features of the copper complex,[26] minimizing electronic repulsion with the CTV unit, could explain the *CTV-in* conformation of Cu^{III}(**Hm-**

Cor). Predominance of such inward conformation in the neutral cage in solution, may also be favoured by entropic factors. In the absence of a guest, a minimized cavity volume is indeed expected to maximize the number of released solvent molecules.[5a] Altogether, experimental characterizations verify the formation of a corrole-based cage of low-symmetry, where the Cu^{III}-corrole core is covalently capped with a CTV unit projecting its convex surface toward the southern corrole unit. Since our efforts to grow single crystals of Cu^{III}(**Hm-Cor**) have remained unsuccessful, its structure has been studied on the basis of DFT calculations. The DFT-optimized structure of Cu^{III}(**Hm-Cor**) confirms the appearance of a well-defined cavity with non-equivalent apertures, described by the southern planar corrole, the northern CTV unit, and the three "side walls" (Figure 2c). A 7.5 Å distance between the Cu-corrole "floor" and the convex face of the CTV "roof" is observed. A cavity displaying one large aperture between the two-opposite biphenyl-based arms (aryl-aryl distance: 14.4 Å), and two more restricted windows (12.2 Å and 11.3 Å aryl-aryl distances), is clearly evidenced.

Fullerene (C_{60} and C_{70}) recognition at Cu^{III}(Hm-Cor).

Having a well-defined cavity with one large entry-window (14.4 Å wall to wall distance, Figure 2c) and two fullerene recognition sites arranged in parallel planes (the CTV[21a] and Cu^{III}corrole units[27]), Cu^{III}(**Hm-Cor**) appears particularly promising for the recognition of fullerenes in a low-symmetry host. In particular, the electron-rich nature of the corrole ligand compared to the porphyrin analogue, appears well-suited to interact with fullerene electron-acceptors.[27] However, Cu^{III}(**Hm-Cor**) displays, in its closed state, an unfavourable orientation of the CTV's concave edge and a short CTV-Cu(corrole) distance (7.5 Å). Benefiting from the conformationally switchable CTV, host-guest assembly between Cu^{III}(**Hm-Cor**) and fullerenes C_{60} and C_{70} might therefore arise from a guest-responsive conformational transformation of the cage. Indeed, DFT-optimized structure of the hypothetic *CTV-out* conformation of the host (Figure 5), reveals a 12 Å CTV-Cu^{III}(Corrole) average distance, well adapted for the encapsulation of fullerene between the CTV's concave surface and the southern Cu^{III}(corrole).[28] The interactions between Cu^{III}(**Hm-Cor**) and fullerenes C_{60} and C_{70} were further investigated. Solution of Cu^{III}(**Hm-Cor**) (2.2 mM) in $CDCl_3$, was stirred with various equivalents of fullerenes (0.35; 0.6; 1.0; 1.5 molar equiv.) for 16 hours at 298 K. In the presence of C_{60}, we observed two sets of cage signals with one set corresponding to the original host and a second set - gradually intensifying over incremental fullerene additions - that could be attributed to $C_{60}\subset Cu^{III}$(**Hm-Cor**) (Figure 4), attesting for the formation of the host-guest complexes in slow exchange on the NMR timescale. Identical results were obtained using C_{70} (Figure S27). Integration of the signal corresponding to both free and complexed cage allows for the calculation of binding constants for C_{60} and C_{70} of K_a = 4290 (± 190) and K_a= 2900 (± 150) respectively. ^{1}H NMR spectrum of $C_{60}\subset Cu^{III}$(**Hm-Cor**) reveals drastic shifts of the CTV resonances compared to the guest-free form of the cage, implying an adjustment of the cavity shape in response to fullerene binding. Signals belonging to the CTV roof clearly indicate a switch from the *CTV-in* to the *CTV-out* state, upon encapsulation of C_{60} (Figures S20-23). $C_{60}\subset Cu^{III}$(**Hm-Cor**) indeed displays downfield-chemical shifts of the resonance belonging to the CTV's aromatic protons ($H_{c,c',c''}$ and $H_{d,d',d''}$) and O-**CH$_3$** protons ($H_{e,e',e''}$) that end up resonating in the characteristic 6.79 – 6.70 and 3.86 – 3.78 ppm regions respectively.

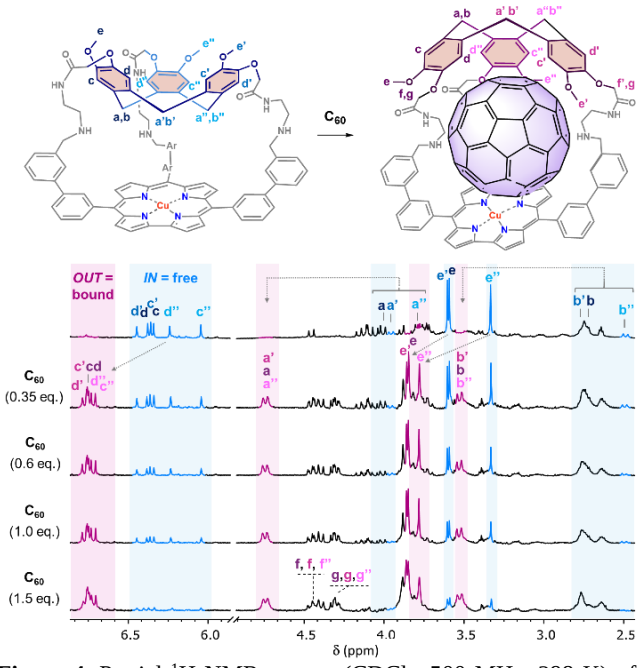

Figure 4. Partial ^{1}H NMR spectra ($CDCl_3$, 500 MHz, 298 K) of Cu^{III}(**Hm-Cor**) upon addition of 0.35; 0.6; 1.0 and 1.5 molar equiv. of C_{60}.

These chemical shifts being consistent with the usual *CTV-out* conformation of hemicryptophane cages (Figure S21). The axial and equatorial methylenic bridging protons ($H_{a,a',a''}$ and $H_{b,b',b''}$), that resonate as six distinct signals in the free cage, merged into two single downfield shifted broad resonances at 4.75 and 3.53 ppm ($\Delta\delta$ = 1.22 ppm with expected COSY and NOESY correlations) in $C_{60}\subset Cu^{III}$(**Hm-Cor**) (Figures S22 and S23). The latter being consistent with the a, a', a'' and b, b', b'' protons pointing toward the outside of the cage and therefore becoming less affected by the low-symmetry inner cavity. Similar behavior is observed with $C_{70}\subset Cu^{III}$(**Hm-Cor**) (Figures S28-30). Furthermore, 2D DOSY NMR spectra of $C_{60}\subset Cu^{III}$(**Hm-Cor**) displays a single diffusion band for each resonance attributed to the host-guest adduct, confirming that these signals belong to a single species (Figure S24). Compared to the original cage (D = 4.9.10^{-10} m^2.s^{-1}), C_{60} host-guest adduct exhibit lower diffusion coefficients (D = 3.9.10^{-10} m^2.s^{-1}). Such increase of the host's volume being in excellent agreement with a switching from the *CTV-in* to the *CTV-out* conformation. UV-vis spectrum of $C_{60}\subset Cu^{III}$(**Hm-Cor**) in CH_2Cl_2, displays the typical signatures of Cu^{III}(**Hm-Cor**) with a slightly shifted Soret band (412 nm) accompanied with the typical absorption of C_{60} at 329 nm (Figure S25). Formation of the 1:1 adduct $C_{60}\subset Cu^{III}$(**Hm-Cor**), was also confirmed *via* high resolution mass spectrometry (ESI-HRMS) analysis (Figure S26). The ability of Cu^{III}(**Hm-Cor**) to accommodate fullerenes in a low-symmetrical cavity was confirmed by the resulting DFT-optimized model for $C_{60}\subset Cu^{III}$(**Hm-Cor**) (Figure 5). Importantly, DFT calculations support the lower stability of the starting host-guest model displaying a closed cage conformation (Figure S53), that converges to the more stable *CTV-out* conformation along structure optimization, confirming that the host indeed adapts its conformation to house the spherical guests.

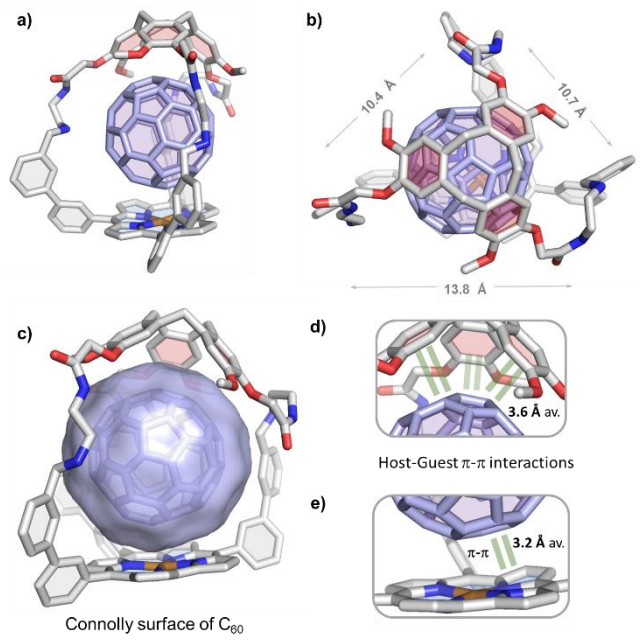

Figure 5. Side (**a**) and top (**b**) views of the DFT optimized structure of C_{60}⊂Cu^{III}(**Hm-Cor**). (**c**) Representation of the C_{60} Connolly surface aiming at visualizing the cavity's occupied volume. Zoom on the CTV to C_{60} (**d**) and corrole to C_{60} (**e**) π-π interactions with average distances.

The DFT-optimized structure reveals excellent size and shape complementarity between C_{60} and the *CTV-out* conformation of the host, as highlighted by visualizing the C_{60} Connolly surface representation, that shows a nearly fully occupied cavity (Figure 5c). Such remarkable spatial complementarity maximizes π-π interactions with the two C_{60} recognizing units with average CTV-C_{60} and corrole-C_{60} distances of 3.6 Å and 3.2 Å respectively. Importantly, the optimal size and shape complementarity between fullerene and the CTV-*out* conformation of Cu^{III}(**Hm-Cor**) was found to be the key to unlocking the cage-opening, leading to the specific binding of spherical fullerene over other common polycyclic aromatic hydrocarbons (PAH) guests. Neither planar coronene nor curved corannulene guests are encapsulated by Cu^{III}(**Hm-Cor**), which remains in its closed state in the presence of excess of these other PAH guests (Figure S32-33). We also demonstrate the selective encapsulation of C_{60} from a mixture containing equimolar equivalents of several PAHs (pyrene, coronene, corannulene, and C_{60}). The cage-opening phenomenon is therefore dictated by the guest's size and shape, allowing for selective binding of fullerene over other PAHs, and representing a key example of conformational opening of an artificial host answering to a specific guest's molecular shape, another common feature of biological receptors.

pH-responsive conformational changes of Cu^{III}(Hm-Cor). It is well established that the electron rich CTV unit efficiently stabilizes ammonium-based guests at its concave edge through cation-π interactions.[25] In addition, self-encapsulation of hemicryptophane side-arms, has been already observed.[29] Accordingly, and considering that the amine-based linkers of Cu^{III}**(Hm-Cor)** could serve as putative pH-responsive moieties,[6a] we reasoned that protonated ammonium (-NH_2^+-) side arms could act as an internal guests. Such -NH_2^+- recognition at the concave CTV surface controlling the *CTV-in* to *CTV-out* molecular motion was supported by DFT-optimized models of [Cu^{III}(**Hm-Cor**) + 3H]$^{3+}$ • 3 CF_3COO^- (Figure 6a). Calculations reveal the lower stability of the closed conformation of the protonated host, which is converging toward the more stable *CTV-out* conformation during the optimization process (Figure S54). Stabilization of one -NH_2^+- moiety via cation-π interactions with the concave surface of the CTV roof is observed in the resulting DFT-optimized structure (Figure 6b). The effect of the secondary amine protonation was then studied upon gradual addition of trifluoroacetic acid (TFA) to a solution of Cu^{III}(**Hm-Cor**) in $CDCl_3$. We focused our attention on the ^{1}H NMR signals belonging to the aromatic ($H_{c,c',c''}$, $H_{d,d',d''}$) and O-**CH_3** ($H_{e,e',e''}$) protons of the CTV unit, that display well-defined and separated resonances. The addition of 1.0 equivalent of TFA, gives rise to a complicated spectrum displaying two sets of signals for each resonance of the CTV units (Figure S34), that could be explained by partial protonation of Cu^{III}(**Hm-Cor**).[30] Further increase of the amount of TFA to 3.0 molar equivalents results in a simpler ^{1}H NMR spectrum displaying a single set of signals for each proton belonging to the CTV unit (Figure 6a). No further changes were observed upon adding additional TFA (4.0 to 6.0 equiv. Figure S34), suggesting that the fully protonated [Cu^{III}(**Hm-Cor**) + 3H]$^{3+}$ is reached after addition of 3.0 equivalents of TFA.

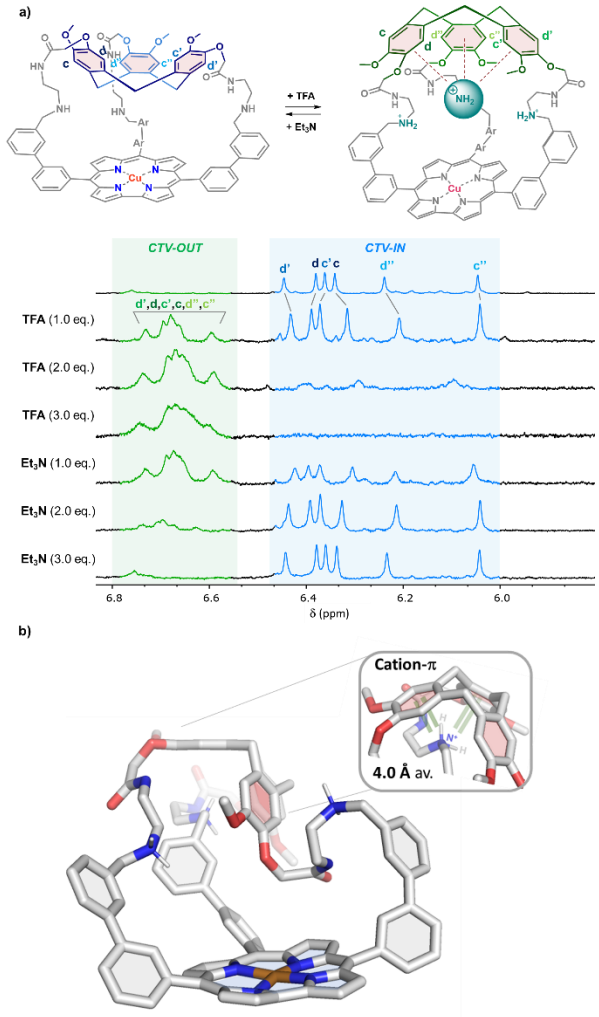

Figure 6. (**a**) Partial ^{1}H NMR spectra (298 K, 400 MHz) of Cu^{III}(**Hm-Cor**) in $CDCl_3$ and upon addition of 1.0, 2.0 and 3.0 molar equiv. of TFA, followed by the addition of 1.0, 2.0 and 3.0 molar equiv. of triethylamine (Et_3N). (**b**) View of the DFT-optimized structure of [Cu^{III}(**Hm-Cor**) + 3H]$^{3+}$ • 3 CF_3COO^- with zoom on the CTV to -NH_2^+- interactions (anions were omitted for clarity).

^{1}H NMR spectrum of the cage in its fully protonated salt form [Cu^{III}(**Hm-Cor**) + 3H]$^{3+}$ • 3 CF_3COO^-, reveals drastic shifts of the resonances belonging to the CTV cap. Compared to the neutral form of the cage, signals of the CTV's aromatic protons $H_{c,c',c''}$ and $H_{d,d',d''}$, undergo, upon protonation, a strong downfield-chemical shift to the 6.6 - 6.75 ppm region.

Similar behaviour is observed with signals belonging to the O-**CH_3** protons of the CTV ($H_{e,e',e''}$, Figure S34). The axial ($H_{a,a',a''}$) and equatorial ($H_{b,b',b''}$) methylenic bridging protons also experience a strong chemical shift and resonate as two broad sets of merged signals ($H_{a,a',a''}$ 4.63 - 4.56 ppm and $H_{b,b',b''}$ 3.13 - 3.10 ppm with expected COSY and NOESY correlations, Figures S38-39). Such changes of the CTV's resonances - that clearly resemble the ones observed upon fullerenes encapsulations - are diagnostic of a pH-responsive conformational switch to *CTV-out*. Subsequent additions of triethylamine (Et_3N, 1.0, 2.0 and 3.0 molar equiv., Figure 6a) lead to restoration of the original chemical shifts of Cu^{III}(**Hm-Cor**), attesting for a reversible interconversion between the *CTV-in* and *CTV-out* conformations. These observations support the hypothesis of a conformational switch toward the *CTV-out* form, driven by cation-π interactions between one internal -NH_2^+- guest and the concave surface of the electron rich CTV.[31] Further support for this conformational switch was provided by DOSY NMR (Figure S42), which revealed that the protonated host shares similar diffusion coefficients as C_{60}⊂Cu^{III}(**Hm-Cor**) (D = 4.3.10^{-10} $m^2.s^{-1}$ and D = 3.9.10^{-10} $m^2.s^{-1}$ respectively). These lower diffusion coefficients, compared to the empty neutral cage (D= 4.9.10^{-10} $m^2.s^{-1}$) are in excellent agreement with the increase of the host's size by switching from *CTV-in* to *CTV-out* conformations upon protonation.

pH-dependent on-demand fullerenes release. Stimuli-responsive uptake/release of guest molecules, without irreversibly disassembling the host, remains a major challenge for the creation of reusable receptors. Furthermore, the on-demand liberation of sequestrated guest is highly valuable to fullerene-based host-guest chemistry,[32] examples of efficient fullerene recognition by reusable hosts being scarce.[33] On these grounds, we wondered if the pH-responsive self-encapsulation of one -NH_2^+- side arm, observed for Cu^{III}(**Hm-Cor**), could promote the ejection of the encapsulated C_{60} *via* intramolecular guest exchange. Interestingly, addition of TFA (3.3 molar equiv., 2 hours stirring) to a solution of C_{60}⊂Cu^{III}(**Hm-Cor**) in a $CDCl_3$/CD_3OD 9:1 solvent mixture, followed by NMR, reveals fullerene's ejection with the disappearance of the signals belonging to the host-guest adduct, to the profit of the signals corresponding to the protonated cage (Figure S48). Identical behaviour was observed using C_{70}⊂Cu^{III}(**Hm-Cor**) (Figure S44). As a control experiment, no change in the ^{1}H NMR spectrum of [Cu^{III}(**Hm-Cor**) + 3H]$^{3+}$ • 3 CF_3COO^- was observed upon addition of C_{60}, confirming that the protonated host did not efficiently interact with fullerenes. Importantly, further addition of Et_3N, to generate the neutral host results in the encapsulation of C_{60} (Figure S45). Although fullerene ejection could be reached upon addition of 3.3 equiv. of TFA (Figure S48), no guest release could be observed upon partial protonation of the host (1.0 or 2.0 equiv. of TFA). The latter being in good agreement with Cu^{III}(**Hm-Cor**) protonation studies, where complete encapsulation of the -NH_2^+- arm (forming the CTV-*out* conformation), was reached with addition of 3 equiv. of acid (Figure 6a).

Finally, the orthogonal solubilities between the protonated cage (soluble in MeOH) and the liberated fullerene (soluble in toluene) have been exploited to isolate and quantify the recovered fullerene and the reusability of the cage. 8 equiv. of TFA were added to a solution of C_{60}⊂Cu^{III}(**Hm-Cor**) or C_{70}⊂Cu^{III}(**Hm-Cor**) in a $CHCl_3$:MeOH 9:1 solvent mixture (2.14 mM). The resulting mixture was stirred for 2 hours at 298 K, evaporated to dryness, and washed with methanol. Remarkably, C_{60} and C_{70} were recovered as insoluble material with 83% and 97% yields, respectively (Figures S46-47). Finally, deprotonation of [Cu^{III}(**Hm-Cor**) + 3H]$^{3+}$ • 3 CF_3COO^- using NaOH, allows recovery of the starting neutral host with 80% isolated yield. The recovered cage was successfully applied to further fullerene recognitions, demonstrating its reusability.

Cu^{III}(Hm-Cor)-protected Diels-Alder (DA) functionalization of C_{60} with pentacene (Pn). The encapsulation of C_{60} with high shape complementarity in a capsule displaying differently sized windows, together with the facile release of fullerene guests upon simple protonation, makes Cu^{III}(**Hm-Cor**) an especially appealing host to be studied as a low-symmetry shadow mask. As proof-of-concept, we sought to demonstrate that selective mono-functionalization of C_{60} with bulky pentacene (Pn) could occur selectively at the larger entry window by exposing C_{60}⊂Cu^{III}(**Hm-Cor**) to a DA reaction with Pn. Identical reactions had been studied previously within symmetrical porphyrin-based cages, leading to the selective formation of the symmetrical *trans-1*-bis-adduct upon reacting caged fullerenes with 2.1 equiv of Pn.[12c,12d] With bare C_{60}, DA reactions necessitates problematic solvents (CS_2, benzene, chlorinated aromatics) and is known to afford mixtures of mono-, bis-, and even double C_{60} adducts[34]).[12c,12d,12e] Conversely, the reaction of C_{60}⊂Cu^{III}(**Hm-Cor**) with 2.5 equiv of Pn in $CDCl_3$ at 50°C in the dark for 16h afforded the pentacene mono-adduct Pn-C_{60} as the sole observable product. Formation of the host guest adduct between Pn-C_{60} and the CTV-*out* conformation of Cu^{III}(**Hm-Cor**), was observed by ^{1}H NMR and ESI-HRMS analysis (Figures S49 and S50). Importantly, ejection of the guest product was successfully achieved by applying our TFA-based fullerene release protocol, which allows the isolation and characterization of Pn-C_{60} as the sole fullerene adduct product (See ESI and Figure S51). To further understand the origin of this selectivity (contrasting with symmetrical porphyrin-based cages, which result in the selective formation of *trans-1*-bis-adduct),[12c] the DFT-optimized structure of Pn-C_{60}⊂Cu^{III}(**Hm-Cor**) was calculated (Figure 7). Importantly, the DFT-optimized structure reveals a selective orientation of the Pn-C_{60} guest, with its Pn moiety "locked" at the larger window (adopting a vertical orientation with respect to the cage). Pn-C_{60}⊂Cu^{III}(**Hm-Cor**) displays one small back window that cannot accommodate the addition of a second Pn due to steric constraints (Figure S55c) along with a medium-sized window exposing one reactive C_{60}'s C-C bond. However, this bond is oriented perpendicularly to the corrole, which implies that the second Pn unit should approach parallel to the macrocycle, which is highly disfavored due to obvious steric clashes between the bulky Pn and the cage linkers (Figure S55b). Cu^{III}(**Hm-Cor**) therefore allows for single orientation of the Pn-C_{60} guests preventing further DA reaction with acene, while preserving putative access at the medium-sized windows for other kind of reactivity with smaller substrates. Noteworthy Cu^{III}(**Hm-Cor**) could also form host-guest adduct with PCBM-C_{60} (PCBM= phenyl-butyric acid methyl ester), the asymmetric C_{60} derivative widely used in material sciences.[35] In this case, no DA reaction between the encapsulated PCBM and Pn (2.5 equiv.) could be observed after two days at 50°C, even though PCBM-C_{60} is known to react with acenes at room temperature

(Figure S52).[36] This result strongly suggests preferential addend positioning with the PCBM group oriented at the larger cage window. Altogether, these findings confirm that Cu^{III}(**Hm-Cor**) could be used to either direct size-dependent reactivity at its larger window or selectively position C_{60} derivatives equipped with bulky substituents.

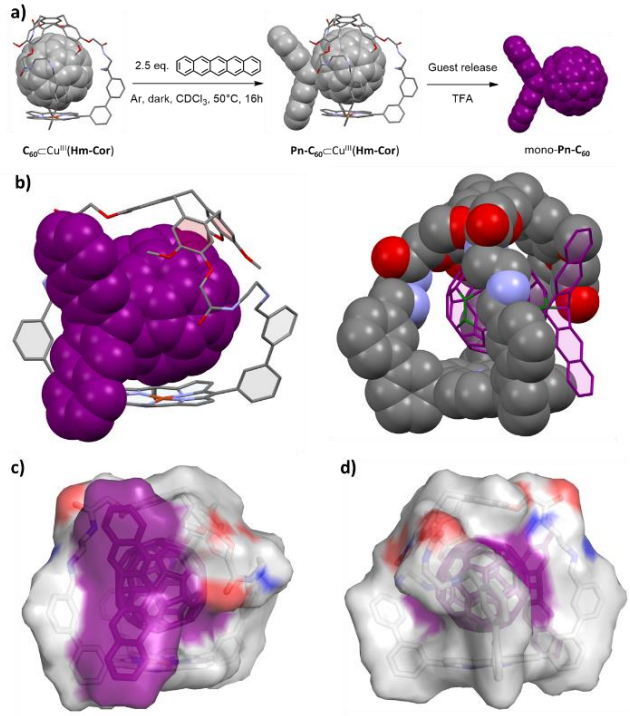

Figure 7. (**a**) Cu^{III}(**Hm-Cor**)-protected Diels-Alder reaction of C_{60} and pentacene (Pn). **b**) Side views of the DFT-optimized structure of **mono-Pn-C$_{60}$**⊂Cu^{III}(**Hm-Cor**). Views of surfaces of **Pn-C$_{60}$** exposed to the outside environment (in purple) at the large front window (**c**) and at the small- and medium-sized back windows (**d**).

CONCLUSION

The peculiar C_{2V} symmetry of metallocorroles make them ideal candidates to deviate from the time-honored D_{4h} porphyrin building blocks and create novel heme-like cavities with non-equivalent apertures. The introduction of a concave–convex shape switching roof into a (Cu^{III})-corrole complex, *via* three pH-responsive side arms, enables the first metallocorrole-based cage Cu^{III}(**Hm-Cor**) to reversibly bind fullerenes in a conformationally adaptive, pH-responsive and low-symmetrical cavity. The relatively large corrole-based foundation enables the CTV roof to act as a guest-responsive switchable recognition unit. From an initial *CTV-in* conformation, where the convex surface of the cap is projected toward the cage interior, the switchable roof could adopt a *CTV-out* conformation enabling selective encapsulation of fullerenes over other planar or curved PAHs. Experimental and computational studies evidence the flipping of the CTV roof upon binding of C_{60} and C_{70} guests, expanding the size of the cavity and providing excellent shape complementarity between spherical fullerenes and the concave π-surface of the CTV. Both CTV and Cu^{III}-corrole units act as recognition sites, breathing life to a unique encapsulation of fullerenes in a desymmetrized cavity with three non-equivalent apertures. Reversible transition between *CTV-in* and *CTV-out* conformations also responds to pH change *via* formation of secondary dialkylammonium (-CH_2-NH_2^+-CH_2-) at the cage's side walls. The protonated form of the cage adopts the *CTV-out* form, to enable stabilization of a secondary ammonium bridging group at the CTV's concave edge, *via* well-known cation-π interactions. This molecular motion - consisting in a self-encapsulation of one protonated side-arm with concomitant CTV flip - could be reversibly controlled through sequential additions of acid and base, revealing a stimuli-responsive cavity. Importantly, once applied to the cage-fullerene adducts, the pH-triggered motion leads to the ejection of the entrapped C_{60} (or C_{70}). This reversible process allowing separation and recovery of both liberated fullerene and starting neutral host, ready to be reused. The encapsulation of C_{60} in a capsule displaying differently sized windows, together with the facile release of entrapped products upon simple protonation, makes Cu^{III}(**Hm-Cor**) an especially appealing host to be studied as a low-symmetry shadow mask. In this line, this work also demonstrated the relevance of the low-symmetrical host to direct DA reactivity between cage-protected C_{60} and pentacene at the larger host's gate, providing dinstinc selectivity than the one previously reached with symmetrical porphyrin-based cages. Cu^{III}(**Hm-Cor**) indeed allows for a preferential orientation of C_{60} adducts at its large window, that prevent further DA reaction with bulky reactants. This unprecedented precise positioning of fullerene derivatives in a reusable low-symmetrical host being particularly appealing for further enantioselective fullerene functionalization.[36]

Inspired by biological receptors, the interest in desymmetrized cage compounds, guest-adaptive shapeshifting cavities, and stimuli responsive (reusable) hosts, is increasing drastically. However, the major challenge remains to combine these features in advanced artificial receptors, increasing their structural and functional complexity. In this report, we therefore establish a key precedent of a single host regrouping these important features. Our synthetical strategy being generalizable across the caging of emerging corrole catalysts,[14,16] this work also opens a valuable perspective in the field of confined space catalysis.

ASSOCIATED CONTENT

Supporting Information. Additional experimental details, materials and methods, procedures, ^{1}H NMR spectra of all compounds, compound characterization data, computational details and host-guest supramolecular complexes informations. "This material is available free of charge *via* the Internet at http://pubs.acs.org."

AUTHOR INFORMATION

Corresponding Authors

Cédric Colomban - Institute of Molecular Sciences of Marseille, 52 Av. Escadrille Normandie Niemen, 13013 Marseille, France. orcid.org/0000-0002-6862-4173 ;
Email : cedric.colomban@univ-amu.fr
Gabriel Canard – CINAM UMR 7325, Campus de Luminy, 13288 Marseille cedex 09, France.
Email : gabriel.canard@univ-amu.fr
Alexandre Martinez - Institute of Molecular Sciences of Marseille, 52 Av. Escadrille Normandie Niemen, 13013 Marseille, France. Email : alexandre.martinez@centrale-marseille.fr
Maylis Orio - Institute of Molecular Sciences of Marseille, 52 Av. Escadrille Normandie Niemen, 13013 Marseille, France.
Email : maylis.orio@univ-amu.fr

ACKNOWLEDGMENT

This work was supported by ANR-22-CE50-0009-01 and the France 2030 investment plan as part of the "*Initiative excellence d'Aix-Marseille Université*" - A*MIDEX (AMX-21-PEP-041). X.R thanks MCIN Spain (PID2022-136970NB-I00) and GenCat for an ICREA Academia award. T.P. thanks MCIN for an FPU grant.

REFERENCES

(1) (a) Morimoto, M.; Bierschen, S. M.; Xia, K. T.; Bergman, R. G.; Raymond, K. N.; Dean Toste, F. Advances in supramolecular host-mediated reactivity. *Nat Catal.* **2020**, DOI:10.1038/s41929-020-00528-3; (b) Syntrivanis, L.-D.; Tiefenbacher, K. Reactivity Inside Molecular Flasks: Acceleration Modes and Types of Selectivity Obtainable. *Angew. Chem. Int. Ed.* **2024**, e202412622; (c) Salazar, A.; Moreno-Simoni, M.; Kumar, S.; Labella, J.; Torres, T.; de la Torre, G. Supramolecular Subphthalocyanine Cage as Catalytic Container for the Functionalization of Fullerenes in Water. *Angew. Chem. Int. Ed.* **2023**, 62, e202311255.

(2) Diao, D.; Simaan, A. J.; Martinez, A.; Colomban, C. Bioinspired complexes confined in well-defined capsules: getting closer to metalloenzyme functionalities. *Chem. Commun.* **2023**, 59, 4288–4299.

(3) Mc Ternan, C. T.; Davies, J. A.; Nitschke, J. R. Beyond Platonic: How to Build Metal–Organic Polyhedra Capable of Binding Low-Symmetry, Information-Rich Molecular Cargoes. *Chem. Rev.* **2022**, 122, 10393–10437.

(4) (a) Bete, S. C.; Otte, M. Heteroleptic Ligation by an endo-Functionalized Cage. *Angew. Chem. Int. Ed.* **2021**, 60, 18582–18586; (b) Andrews, K. G.; Horton, P. N.; Coles, S. J. Programmable synthesis of organic cages with reduced symmetry. *Chem. Sci.* **2024**, 15, 6536–6543; (c) Yang, Y.; Ronson, T. K.; Teeuwen, P. C. P.; Du, Y.; Zheng, J.; Wales, D. J.; Nitschke, J. R. Guest binding is governed by multiple stimuli in low-symmetry metal-organic cages containing bis-pyridyl(imine) vertices. *Chem* **2024**, DOI: 10.1016/j.chempr.2024.08.011; (d) Parbin, M.; Sivalingam, V.; Chand, D. K. Highly Anisotropic $Pd_2L^{ab}{}_2L^{cc}{}_2$ and $Pd_2L^{ab}{}_2L^{cd}{}_2$ Type Cages by Heteromeric Completive Self-Sorting. *Angew. Chem. Int. Ed.* **2024**, e202410219; (e) Faulkner, L. A. V.; Crowley, J. D. The beauty of low symmetry: Non-statistical assembly of $[Pd_2(L_A)(L_B)(L_C)(L_D)]^{4+}$ cages. *Chem* **2024**, 2, 440-442; (f) Prajapati, D.; Clegg, J. K.; Mukherjee, P. S. Formation of a low-symmetry Pd_8 molecular barrel employing a hetero donor tetradentate ligand, and its use in the binding and extraction of C_{70}. *Chem. Sci.* **2024**, 15, 12502–12510. (g) Shi, J.; Wang, M. Construction and Function of Low-Symmetry Metallo-Supramolecules. *Acc. Chem. Res.* **2025**, 58, 1893−1902. (h) Guo, X.-Q.; Yu, P.; Zhou, L.-P.; Hu, S.-J.; Duan, X.-F.; Cai, L.-X.; Bao, L.; Lu X.; Sun, Q.-F. Low-symmetry coordination cages enable recognition specificity and selective enrichment of higher fullerene isomers. *Nat. Synth.* **2025**, 4, 359–369.

(5) (a) Xu, H.; Ronson, T. K.; Heard, A. W.; Teeuwen, P. C. P.; Schneider, L.; Pracht, P.; Thoburn, J. D.; Wales, D. J.; Nitschke, J. R. A pseudo-cubic metal–organic cage with conformationally switchable faces for dynamically adaptive guest encapsulation. *Nat. Chem.* **2025**, 17, 289–296; (b) Gia, A. P.; de Juan, A.; Aranda, D.; Guijarro, F. G.; Aragó, J.; Ortí, E.; García-Iglesias, M.; González-Rodríguez, D. Highly Rigid, Yet Conformationally Adaptable, Bisporphyrin sp^2-Cage Receptors Afford Outstanding Binding Affinities, Chelate Cooperativities, and Substrate Selectivities. *J. Am. Chem. Soc.* **2025**, 147, 1, 918–931; (c) Tamura, Y.; Takezawa, H.; Fujita, M. A Double-Walled Knotted Cage for Guest-Adaptive Molecular Recognition. *J. Am. Chem. Soc.* **2020**, 142, 5504−5508; (d) Wang, J.; Ju, Y.-Y.; Low, K.-H.; Tan, Y.-Z.; Liu, J. A Molecular Transformer: A π-Conjugated Macrocycle as an Adaptable Host. *Angew. Chem. Int. Ed.* **2021**, 60, 11814 –11818.

(6) (a) Pang, X.-Y.; Zhou, H.; Xie, X.; Jiang, W.; Yang, Y.; Sessler, J. L.; Gong, H.-Y. 1,3,5–2,4,6-Functionalized Benzene Molecular Cage: An Environmentally Responsive Scaffold that Supports Hierarchical Superstructures. *Angew. Chem. Int. Ed.* **2024**, e202407805; (b) Pearcy, A. C.; Lisboa, L. S.; Preston, D.; Page, N. B.; Lawrence, T.; Wright, L. J.; Hartinger, C. G.; Crowley, J. D. Exploiting reduced-symmetry ligands with pyridyl and imidazole donors to construct a second-generation stimuli-responsive heterobimetallic $[PdPtL_4]^{4+}$ cage. *Chem. Sci.* **2023**, 14, 8615–8623; (c) Goeb, S.; Sallé, M. Electron-rich Coordination Receptors Based on Tetrathiafulvalene Derivatives: Controlling the Host–Guest Binding. *Acc. Chem. Res.* **2021**, 54, 4, 1043–1055; (d) Krykun, S.; Dekhtiarenko, M.; Canevet, D.; Carré, V.; Aubriet, F.; Levillain, E.; Allain, M.; Voitenko, Z.; Sallé, M.; Goeb, S. Metalla-Assembled Electron-Rich Tweezers: Redox-Controlled Guest Release Through Supramolecular Dimerization. *Angew. Chem. Int. Ed.* **2020**, 59, 716 –720; (e) Colomban, C.; Szalóki, G.; Allain, M.; Gomez, L.; Goeb, S.; Sallé, M.; Costas, M.; Ribas, X. Reversible C_{60} Ejection from a Metallocage through the Redox-Dependent Binding of a Competitive Guest. *Chem. Eur. J.* **2017**, 23, 3016 – 3022.

(7) Pullen, S.; Tessarolo, J.; Clever, G. H. Increasing structural and functional complexity in self-assembled coordination cages. *Chem. Sci.* **2021**, 12, 7269–7293.

(8) (a) Elemans, J. A. A. W.; Nolte, R. J. M. Porphyrin cage compounds based on glycoluril – from enzyme mimics to functional molecular machines. *Chem. Commun.* **2019**, 55, 9590-9605; (b) Ouyang, J.; Swartjes, A.; Geerts, M.; Gilissen, P. J.; Wang, D.; Teeuwen, P. C. P.; Tinnemans, P.; Vanthuyne, N.; Chentouf, S.; Rutjes, F. P. J. T.; Naubron, J.-V.; Crassous, J.; Eleman, J. A. A. W.; Nolte, R. J. M. Absolute configuration and host-guest binding of chiral porphyrin-cages by a combined chiroptical and theoretical approach. *Nat. Commun.* **2020**, 1, 4776; (c) Yang, X.; Ullah, Z.; Stoddart, J. F.; Yavuz, C. T. Porous Organic Cages. *Chem. Rev.* **2023**, 123, 8, 4602–4634.

(9) (a) Surendran, A. K.; Tripodi, G. L.; Pluharová, E.; Pereverzev, A. Y.; Bruekers, J. P. J.; Elemans, J. A. A. W.; Meijer, E. J.; Roithová, J. Host-guest tuning of the CO_2 reduction activity of an iron porphyrin cage. *Nat. Sci.* **2022**, e20220019. (b) García-Simón, C.; G.-Doria, R.; Raoufmoghaddam, S.; Parella, T.; Costas, M.; Ribas, X.; Reek, J. N. H. Enantioselective Hydroformylation by a Rh-Catalyst Entrapped in a Supramolecular Metallocage. *J. Am. Chem. Soc.* **2015**, 137, 2680−2687.

(10) (a) Durot, S.; Taesch, J.; Heitz, V. Multiporphyrinic cages: architectures and functions. *Chem. Rev.* **2014**, 114, 8542−8578; (b) Mukhopadhyay, R. D.; Kim, Y.; Koo, J.; Kim, K. Porphyrin Boxes. *Acc. Chem. Res.* **2018**, 51, 2730−2738.

(11) (a) García-Simón, C.; Colomban, C.; Aybars Çetin, Y.; Gimeno, A.; Pujals, M.; Ubasart, E.; Fuertes-Espinosa, C.; Asad, K.; Chronakis, N.; Costas, M.; Jiménez-Barbero, J.; Feixas, F.; Ribas, X. Complete Dynamic Reconstruction of C_{60}, C_{70}, and $(C_{59}N)_2$ Encapsulation into an Adaptable Supramolecular Nanocapsule. *J. Am. Chem. Soc.* **2020**, 142, 16051−16063; (b) Zhang, C.; Wang, Q.; Long, H.; Zhang, W. A Highly C_{70} Selective Shape-Persistent Rectangular Prism Constructed through One-Step Alkyne Metathesis. *J. Am. Chem. Soc.* **2011**, 133, 20995–21001.

(12) (a) Chang, X.; Xu, Y.; von Delius, M. Recent advances in supramolecular fullerene chemistry. *Chem. Soc. Rev.* **2024**, 53, 47–83; b) Ubasart, E.; Borodin, O.; Fuertes-Espinosa, C.; Xu, Y.; García-Simón, C.; Gómez, L.; Juanhuix, J.; Gándara, F.; Imaz, I.; Maspoch, D.; von Delius, M.; Ribas, X. A three-shell supramolecular complex enables the symmetry-mismatched chemo- and regioselective bis-functionalization of C_{60}. *Nat. Chem.* **2021**, 13, 420–427. (c) Pujals, M. ; Pèlachs, T. ; Fuertes-Espinosa, C. ; Parella, T. ; Garcia-Borràs, M. ; Ribas, X. Regioselective access to orthogonal Diels-Alder C_{60} bis-adducts and tris-heteroadducts via supramolecular mask strategy *Cell Rep. Phys. Sci*. **2022**, 3, 100992. (d) Pèlachs, T.; Sabrià, C.; Iannace, V.; Imaz, I.; Gándara, F.; Maspoch, D.; Feixas, F.; Ribas X. Supramolecular Mask Regioconverter: Orthogonal Diels–Alder C_{70} Bisadducts by Mask-

Mediated Regioselective Synthesis, *CCS Chem.* **2025**, 7, 703–715. (e) Chen, B.; Holstein, J. J.; Horiuchi, S.; Hiller, W. G.; Clever, G. H. Pd(II) Coordination Sphere Engineering: Pyridine Cages, Quinoline Bowls, and Heteroleptic Pills Binding One or Two Fullerenes, *J. Am. Chem. Soc.* **2019**, 141, 8907−8913.

(13) Although corroles are non-natural ligands, their structure reproduces the corrin type skeleton found in the vitamin B12 cofactor and possess aromaticity that confer electronic properties similar to those of heme.

(14) (a) Di Natale, C.; Gros, C. P.; Paolesse, R. Corroles at work: a small macrocycle for great applications. *Chem. Soc. Rev.* **2022**, 51, 1277–1335; (b) Sacramento, J. J. D.; Albert, T.; Siegler, M.; Moënne-Loccoz, P.; Goldberg, D. P. An Iron(III) Superoxide Corrole from Iron(II) and Dioxygen. *Angew. Chem. Int. Ed.* **2022**, 61, e202111492; (c) De, R.; Gonglach, S.; Paul, S.; Haas, M.; Sreejith, S. S.; Gerschel, P.; Apfel, U.-P.; Huyen Vuong, T.; Rabeah, J.; Roy, S.; Schçfberger, W. Electrocatalytic Reduction of CO_2 to Acetic Acid by a Molecular Manganese Corrole Complex. *Angew. Chem. Int. Ed.* **2020**, 59, 10527 – 10534.

(15) (a) Kumar, A.; Kim, D.; Kumar, S.; Mahammed, A.; Churchill, D. G.; Gross, Z. Milestones in corrole chemistry: historical ligand syntheses and post-functionalization. *Chem. Soc. Rev.* **2023**, 52, 573–600; (b) Orłowski, R.; Gryko, D.; Gryko, D. T. Synthesis of Corroles and Their Heteroanalogs. *Chem. Rev.* **2017**, 117, 3102−3137.

(16) Xu, Y.; Jin, X.; Zhang, J.; Qin, H.; Mei, B.; Liu, T.; Lei, S.; Li, S.; Bo, Y.; Li, X.; Cao, R. Regulating Steric Effect of Cobalt Corroles for Promoted Oxygen Electrocatalysis. *ACS Catal.* **2024**, 14, 14350−14355.

(17) (a) Collman, J. P.; Decréau, R. A. 5,10,15-Tris(*o*-aminophenyl) Corrole (TAPC) as a Versatile Synthon for the Preparation of Corrole-Based Hemoprotein Analogs. *Org. Lett.* **2005**, 7, 975−978; (b) Andrioletti, B.; Rose, E. Synthesis of the first superstructured chiral corrole. *J. Chem. Soc. Perkin Trans.* **2002**, 1, 715−716.

(18) Lei, H.; Zhang, Q.; Liang, Z.; Guo, H.; Wang, Y. ; Lv, H.; Li, X.; Zhang, W.; Apfel, U.-P.; Cao, R. Metal-Corrole-Based Porous Organic Polymers for Electrocatalytic Oxygen Reduction and Evolution Reactions. *Angew. Chem. Int. Ed.* **2022**, 61, e202201104.

(19) Thorp-Greenwood, F. L.; Howard, M. J.; Kuhn, L. T.; Hardie, M. J. Fully Collapsed Imploded Cryptophanes in Solution and in the Solid State. *Chem. Eur. J.* **2019**, 25, 3536 – 3540.

(20) Miton, L.; Antonetti, E.; García-López, D.; Nava, P.; Robert, V.; Albalat, M.; Vanthuyne, N.; Martinez, A.; Cotelle, Y. A Cyclotriveratrylene Solvent-Dependent Chiral Switch. *Chem. Eur. J.* **2024**, 30, e202303294.

(21) (a) Huerta, E.; Metselaar, G. A.; Fragoso, A.; Santos, E.; Bo, C.; de Mendoza, J. Selective Binding and Easy Separation of C_{70} by Nanoscale Self-Assembled Capsules. *Angew. Chem. Int. Ed.* **2007**, 46, 202 –205; (b) Huerta, E.; Isla, H.; Pérez, E. M.; Bo, C.; Martin, N.; de Mendoza, J. Tripodal exTTF-CTV Hosts for Fullerenes. *J. Am. Chem. Soc.* **2010**, 132, 5351–5353.

(22) Paolesse, R.; Nardis, S.; Sagone, F.; Khoury, R. G. Synthesis and Functionalization of *meso*-Aryl-Substituted Corroles. *J. Org. Chem.* **2001**, 66, 2, 550-556.

(23) (a) Wasbotten, I. H.; Wondimagegn, T.; Ghosh, A. Electronic Absorption, Resonance Raman, and Electrochemical Studies of Planar and Saddled Copper(III) *meso*-Triarylcorroles. Highly Substituent-Sensitive Soret Bands as a Distinctive Feature of High-Valent Transition Metal Corroles. *J. Am. Chem. Soc.* **2002**, 124, 8104-8116; (b) Alemayehu, A. B.; Gonzalez, E.; Kristian Hansen, L.; Ghosh, A. Copper Corroles Are Inherently Saddled. *Inorg. Chem.* **2009**, 48, 7794–7799.

(24) The reductive amination reaction (formation of the imine bond prior to its *in-situ* sodium borohydride reduction) was performed under diluted conditions (1mM).

(25) Zhang, D.; Martinez, A.; Dutasta, J.-P. Emergence of Hemicryptophanes: From Synthesis to Applications for Recognition, Molecular Machines, and Supramolecular Catalysis. *Chem. Rev.* **2017**, 117, 4900–4942.

(26) Ngo, T. H.; Zieba, D.; Webre, W. A.; Lim, G. N.; Karr, P. A.; Kord, S.; Jin, S.; Ariga, K.; Galli, M.; Goldup, S.; Hill, J. P.; D'Souza, F. Engaging Copper(III) Corrole as an Electron Acceptor: Photoinduced Charge Separation in Zinc Porphyrin–Copper Corrole Donor–Acceptor Conjugates. *Chem. Eur. J.* **2016**, 22, 1301 – 1312.

(27) Chen, C.; Zhu, Y.-Z.; Fan, Q.-J.; Song, H.-B.; Zheng, J.-Y. Syntheses of corrole derivatives and their supramolecular interactions with fullerenes in solution and the solid state. *Tetrahedron Letters* **2013**, 54, 4143–4147.

(28) Ku, M.-Y.; Huang, S.-J.; Huang, S.-L.; Liu, Y.-H.; Lai, C.-C; Peng, S.-M.; Chiu, S.-H. Hemicarceplex formation allows ready identification of the isomers of the metallofullerene $Sc_3N@C_{80}$ using ^1H and ^{13}C NMR spectroscopy. *Chem. Commun.* **2014**, 50, 11709-11712.

(29) Qiu, G.; Colomban, C.; Vanthuyne, N.; Giorgi, M.; Martinez, A. Chirality transfer in a cage controls the clockwise/anticlockwise propeller arrangement of the tris(2-pyridylmethyl)amine ligand. *Chem. Commun.* **2019**, 55, 14158-14161.

(30) A first contribution for the aromatic CTV's protons (Hc,c',c", Hd,d',d"), that resemble the spectrum of Cu^{III}(**Hm-Cor**) with slightly shifted resonances between 6.0 and 6.5 ppm, could be assigned to a partially protonated *CTV-in* conformation of the cage. A second signals set could be observed in the 6.6 to 6.75 ppm range, evidencing a conformational change. Identical behaviour could be observed for the CTV's methoxy protons (He,e',e").

(31)A binding of the trifluoroacetate couterions at the protonated cage (Avery, Z. T; Elphick, E. C.; Gardiner, M. G.; Goodwin, R. J.; Ho, J.; Peeks, M. D.; Preston, D. Dual Proton/Anion Binding Through Reciprocal Allostery in Platinum(II) Lantern-Shaped Cages, *Angew. Chem. Int. Ed.* **2025**, e21306) was excluded by ^{19}F-NMR analysis of $[Cu^{III}$(**Hm-Cor**$) + 3H]^{3+}$ • 3 CF_3COO^- that reveal a single resonance for the three CF_3COO^- anion (without significant shifts compared to the free anion), ruling-out the possibility of an anion-promoted conformational change.

(32) Garcia-Simon, C.; Garcia-Borras, M.; Gomez, L.; Parella, T.; Osuna, S.; Juanhuix, J.; Imaz, I.; Maspoch, D.; Costas, M.; Ribas, X. Sponge-like molecular cage for purification of fullerenes. *Nat. Commun.* **2014**, 5, 5557.

(33) Ibáñez, S.; Mejuto, C.; Cerón, K.; Sanz-Miguel, P. J.; Peris, E. A corannulene-based metallobox for the encapsulation of fullerenes. *Chem. Sci.* **2024**, 15, 13415–13420.

(34) Murata, Y.; Kato, N.; Fujiwara, K.; Komatsu, K. Solid-State [4 + 2] Cycloaddition of Fullerene C_{60} with Condensed Aromatics Using a High-Speed Vibration Milling Technique. *J. Org. Chem.* **1999,** *64*, 3483-3488.

(35) Xie, J. ; Li, X. ; Du, Z. ; Liu Y. ; Zhu K. C–H···S Hydrogen Bond Assisted Supramolecular Encapsulation of Fullerenes with Nanobelts. *CCS Chem.* **2023**, 5, 958–970.

(36) Lu, Z.; Ronson, T. K.; Heard, A. W.; Feldmann, S.; Vanthuyne, N.; Martinez, A.; Nitschke, J. R. Enantioselective fullerene functionalization through stereochemical information transfer from a self-assembled cage. *Nat. Chem.* **2023**, 15, 405–412.

Insert Table of Contents artwork here

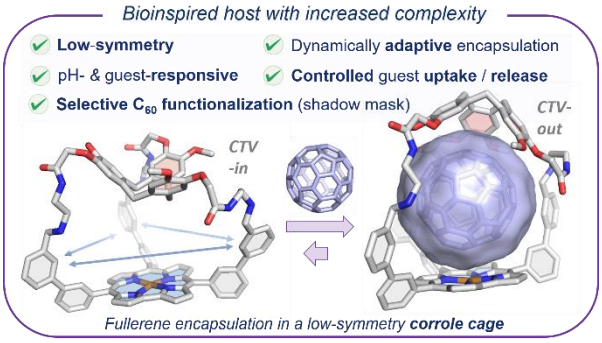

A key precedent for one artificial host regrouping some major features of biological receptors was evidenced.